Plant Soil (2009) 325:39–51
DOI 10.1007/s11104-009-0045-7

REGULAR ARTICLE

In vivo analysis of metal distribution and expression of metal transporters in rice seed during germination process by microarray and X-ray Fluorescence Imaging of Fe, Zn, Mn, and Cu

Michiko Takahashi · Tomoko Nozoye · Nobuyuki Kitajima · Naoki Fukuda · Akiko Hokura · Yasuko Terada · Izumi Nakai · Yasuhiro Ishimaru · Takanori Kobayashi · Hiromi Nakanishi · Naoko K Nishizawa

Received: 8 March 2009 / Accepted: 19 May 2009 / Published online: 20 June 2009

Abstract To investigate the flow of the metal nutrients iron (Fe), zinc (Zn), manganese (Mn), and copper (Cu) during rice seed germination, we performed microarray analysis to examine the expression of genes involved in metal transport. Many kinds of metal transporter genes were strongly expressed and their expression levels changed during rice seed germination. We found that metal transporter genes such as ZIP family has tendency to decrease in their expressions during seed germination. Furthermore, imaging of the distribution of elements (Fe, Mn, Zn, and Cu) was carried out using Synchrotron-based X-ray microfluorescence at the Super Photon ring-8 GeV (SPring-8) facility. The change in the distribution of each element in the seeds following germination was observed by in vivo monitoring. Iron, Mn, Zn, and Cu accumulated in the endosperm and embryos of rice seeds, and their distribution changed during rice seed germination. The change in the patterns of mineral localization during germination was different among the elements observed.

Responsible Editor: Jian Feng Ma.

Michiko Takahashi and Tomoko Nozoye have contributed equally to this work.

M. Takahashi · T. Nozoye · Y. Ishimaru · T. Kobayashi · H. Nakanishi · N. K Nishizawa
Graduate School of Agricultural and life Sciences,
The University of Tokyo,
Yayoi 1-1-1,
Bunkyo-ku, Tokyo 113-8657, Japan

N. Kitajima
Fujita Corporation,
Ono 2025-1,
Atugi-shi, Kanagawa 243-0125, Japan

N. Fukuda · A. Hokura · I. Nakai
Department of Applied Chemistry,
Tokyo University of Science,
1-3, Kagurazaka,
Shinjuku, Tokyo 162-8601, Japan

Y. Terada
SPring-8, JASRI,
Kouto 1-1-1, Sayo-cho,
Sayo-gun, Hyogo 679-5198, Japan

N. K Nishizawa (✉)
Laboratory of Plant Biotechnology,
Department of Global Agricultural Sciences,
The University of Tokyo,
Yayoi 1-1-1,
Bunkyo-ku, Tokyo 113-8657, Japan
e-mail: annaoko@mail.ecc.u-tokyo.ac.jp

Keywords Germination · Rice seed · Transporter · Synchrotron-based X-ray microfluorescence · Metal nutrients

Abbreviations

SPring-8	Super photon ring-8 GeV facility
MAs	Mugineic acid family phytosiderophores
NA	Nicotianamine
DMA	Deoxymugineic acid
FZP	Fresnel zone plate
FWHM	Full-width at half-maxumum
PCR	Oilymerase chain reaction
GUS	β-glucronidase

Introduction

Metal nutrients, such as iron (Fe), manganese (Mn), zinc (Zn), and copper (Cu), are essential for normal plant growth. Fe can be readily reduced or oxidized in biochemical reactions, making it well suited for its role in redox active proteins involved in respiration, photosynthesis, and nitrogen fixation (Hell and Stephan 2003). Fe is also vital for completion of the citric acid cycle, assimilation of sulfur and nitrogen, and chlorophyll biosynthesis. Zn is an important structural component of protein domains such as the Zn-fingers found in many DNA-binding proteins, as well as enzymes such as alcohol dehydrogenase. During seed germination, drastic biological changes occur (Hoshikawa 1973). During rice seed germination, the nutrients stored in the seed are used for germination. The rice seed is composed mainly of embryo and endosperm and the metal nutrients are stored in both structures. An adequate flow of metal elements during seed germination is important for normal growth, but our understanding about the flow dynamics of these metal nutrients during rice seed germination is very limited.

Extensive regulatory cross talk is to be expected between the transition metal homeostasis network and the homeostatic systems of other nutrients (Huang et al. 2000). Maintaining availability and controlling the distribution of metal elements in a plant requires tight control of their transport across membranes and binding to organic and inorganic compounds (Finney and O'Halloran 2003). These plant metal transporter families and their biological roles have been reviewed (Pittman 2005; Williams and Mills 2005; Clemens 2006; Colangelo and Guerinot 2006; Grotz and Guerinot 2006; Hydon and Cobbett 2007; Krämer et al. 2007; Puig et al. 2007).

Synchrotron-based X-ray microfluorescenece (μ-XRE) is a technique well suited to the localization of essential elements in cells and tissues. Most inorganic element biochemistry studies rely to some extent on bulk analysis of the elements of interest. Direct chemical element imaging is often more reliable than bulk analysis because it is not affected by sample preparation, which may alter metal distribution. In addition, chemical element imaging enables us to correlate tissue distribution with biochemical functions, or alteration of these functions. Trace element analysis requires the use of a technique that has detection limits as low as a few micrograms per gram. Direct chemical element imaging has unprecedented detection limits compared to more conventional chemical imaging using electron microscopy (>100 μg/g). In addition, direct chemical element imaging can detect all elements, which is not possible using radioisotopes.

To examine metal flow during rice seed germination, we performed microarray analysis using mRNA extracted from germinating rice seeds, and found that many kinds of transporter genes involved in metal transport were strongly expressed and that their expression levels changed during seed germination. Furthermore, we examined the localization of the endogenous elements (Fe, Zn, Mn, and Cu) in rice seeds during germination using synchrotron-based X-ray microfluorescence (μ-XRF) at the Super Photon ring-8GeV (SPring-8) facility. The localization of Fe, Zn, Mn, and Cu was different from each other, and changed during seed germination. Using promoter–GUS analysis, we showed that the expression patterns of *OsZIP4*, a Zn transporter (Ishimaru et al. 2006), were similar to Zn localization in germinating rice seeds. Our data suggested that metal elements are dynamically mobilized to regions of embryonic growth during rice seed germination.

Material and methods

RNA extraction

Fifty ungerminated seeds and 50 seeds sown on Murashige and Skoog (MS) medium were collected and homogenized separately using MULTI-BEADS

Shocker (Yasui-kikai, Osaka, Japan). RNA was isolated from fully mature and germinating seeds as described by Takaiwa et al. (1987). The RNA was purified using RNeasy mini columns (Qiagen, Tokyo, Japan) following the manufacturer's instructions and used for microarray analysis.

Oligo DNA microarray analysis

A rice 22 K custom oligo DNA microarray kit (Agilent Technologies, Palo Alto, CA, USA), which contains approximately 22,000 oligonucleotides synthesized based on sequence data from the rice full-length cDNA project (http://cdna01.dna.affrc.go.jp/cDNA/), was used. The oligonucleotides were designed using the 3′-non-coding region of each full-length rice cDNA to detect gene-specific expression (www.agilent.com). The RNA yield and purity of the seeds and Fe-sufficient and -deficient shoots and roots were determined spectrophotometrically, and the integrity of the RNA was checked using an Agilent 2100 Bioanalyzer (Agilent Technologies). Hybridization was performed according to the manufacturer's instructions. cDNAs were synthesized from total RNA (1 μg) and labeled with the fluorescent dye Cy3 or Cy5 using an Agilent Low RNA Input Fluorescent Linear Amplification Kit (Agilent Technologies). The fluorescently-labeled targets were then hybridized to the Agilent rice 22 K oligo DNA microarrays. The hybridized microarrays were scanned using an Agilent Microarray Scanner, and extraction software (Feature Extraction version 7.1; Agilent Technologies) was used for image analysis and data extraction. For the microarray analysis, two hybridizations with reciprocally exchanged labeling dyes were performed with two independent biological samples. To detect genes whose expression levels changed during seed germination, the signal intensities from the labeled targets derived from germinating seeds 1–3 days after sowing were compared with those of fully mature seeds (0 days). The microarray results were filtered to select candidate clones with *P*-value log ratios of less than 0.001. A twofold expression cutoff was applied, and cases in which all four replications passed this cutoff were scored as differential expression.

Synchrotron-based X-ray microfluorescence (μ-XRE)

Oryza sativa L. cv. Nipponbare was used for synchrotron-based X-ray microfluorescence. Plants were grown on agar plates without nutrients, and harvested at 12 h, 24 h, and 36 h after sowing. The rice seeds were cut with a vertical slicer into about 100-μm sections, freeze-dried, and used for synchrotron-based X-ray microfluorescence. The in vivo μ-XRE imaging was carried out at BL37XU of the Super Photon ring-8 GeV (SPring-8) facility (Hyogo, Japan; Hokura et al. 2006). Elemental maps were obtained by scanning the samples with a 10.0-keV monochromatic beam. The X-ray beam was focused with a Fresnel Zone Plate (FZP) to a beam size of 0.8 μm (V)×1.4 μm (H) full-width at half-maximum (FWHM), while recording the X-ray fluorescence with a Si (Li) solid-state detector. The FZP was produced by the sputtered-slice manufacturing method (Kamijo et al. 2003). The step size was set to 50 μm (for whole seed) or 10 μm (for embryo) and provided some over-sampling, ensuring that no part of the target was missed. The integrated XRE intensity of each line was calculated from the spectrum and normalized to that of the incident bean, which was measured by an ionization chamber, and then the elemental map of the measured area was calculated.

Rice transformation

Genomic sequences containing the putative promoter regions of *OsZIP4* (–3,000 bp to –1 bp from the translation initiation codon) were amplified from genomic DNA by the polymerase chain reaction (PCR) (Ishimaru et al. 2006). The DNA fragments of the entire promoter region were then fused upstream of the open reading frame of the *uidA* gene, which encodes *GUS*, in the pIG121Hm vector (Hiei et al. 1994). *Agrobacterium tumefaciens* (C58) carrying a binary vector was used to transform rice following the method of Higuchi et al. (2001).

Histochemical analysis

Histochemical assays for GUS activity were conducted according to Jefferson et al. (1987), with some modifications. First, the transgenic seeds were cut in half with a scalpel prior to incubation in the substrate solution. The plant material was fixed in 90% (v/v) acetone for 5 min and rinsed in a buffer containing 50 mM $NaPO_4$ (pH 7.2), 0.5 mM $K_3Fe(CN)_6$, and 0.5 mM $K_4Fe(CN)_6$. GUS staining was performed using 4 mM 5-bromo-4-chloro-3-indolyl-β-glucuronide

(GUS) in staining buffer [50 mM $NaPO_4$ (pH 7.2), 0.5 mM $K_3Fe(CN)_6$, 0.5 mM $K_4Fe(CN)_6$, and 20% methanol] with vacuum infiltration for 30 min on ice, followed by incubation at 37°C in darkness for 24 h. GUS staining was observed under a substance microscope (B061; Olympus, Tokyo, Japan). Each assay was performed at least three times using more than three plant lines.

Results

Expression patterns of transporter genes involved in metal transport

Using the 22 K oligo array, expression profiles of transporter genes were analyzed during rice seed germination (Fig. 1). mRNA extracted from mature rice seeds or seeds 1, 2, and 3, days after sowing were used for oligo array analysis. We examined the expression patterns of the metal transporters, which were previously reported (reviewed in Pittman 2005; Williams and Mills 2005; Clemens 2006; Colangelo and Guerinot 2006; Grotz and Guerinot 2006; Hydon and Cobbett 2007; Krämer et al. 2007; Puig et al. 2007). First, the genes whose signal intensities during seed germination were greater than 1,000 were labeled as having a high level during this stage (Fig. 1, yellow). Second, the transcriptional levels of seeds 1 day, 2 days, and 3 days after sowing were compared with those of fully mature seeds (0 days) (Fig. 1, red, upregulated; blue, downregulated). These data made it possible to calculate the level of gene expression at each stage relative to that in fully ripened seeds, and therefore to understand the temporal changes in the mRNA levels.

The expression levels of the zinc-regulated transporter and the iron-regulated transporter protein (ZIP) family (Eide et al. 1996; Korshunova et al. 1999; Vert et al. 2002; Ishimaru et al. 2006) tended to decrease upon germination (also observed by Nozoye et al. 2007). A member of the cation diffusion facilitator (CDF) family (Williams et al. 2000), the P_{1B}-type ATPase family (Mills et al. 2003), the oligopeptide transporter (OPT) superfamily (Curie et al. 2001), the iron-regulated protein (IREG) family (McKie et al. 2000; Schaaf et al. 2006), IDI7, an Fe deficiency-induced ABC transporter identified in barley (Yamagichi et al. 2002), PIC1, an Fe transporter in the chloroplast (Duy et al. 2007), and the copper transporter (COPT) family (Kampfenkel et al. 1995) were strongly expressed and their expression levels tended to be upregulated during germination (Fig. 1). Rice homologs of the Ca^{2+}-sensitive cross complementer 1 (CCC1) family (OsVIT1: Kim et al. 2006), RAN1 (AtHMA7) belonging to the P-type ATPase subfamily (Hirayama et al. 1999; Woeste and Kieber 2000), Ferric Reductase Defective 3 (FRD3), a citrate transporter of the large multidrug and toxin efflux (MATE) family (Durrett et al. 2007), PAA1 (AtHMA6), the P-type ATPase involved in Cu transfer across the chloroplast envelope (Shikanai et al. 2003), and ECA1, a member of the P-type ATPase subfamily transporting Mn^{2+} (Axelaen and Palmgren 2001) were not strongly expressed and showed no pronounced changes in their expression levels during germination.

To clarify what was happening during rice seed germination, we also compiled a list of the genes whose expression levels (signal intensities) were the highest in mature seeds or seeds 1–3 days after sowing (Table 1); those with the highest ratios in seeds 1 day, 2 days, and 3 days after sowing were compared to mature seeds (Table 2). A gene encoding a seed storage protein was included in the list with the highest signal intensities in the mature seeds and in seeds 1 day after sowing (Table 1). It also included the gene annotated as a Zn-induced protein. Expression of these genes decreased dramatically during seed germination. By 2–3 days after sowing, the signal intensities for several genes increased during seed germination. Metallothionein was included among these genes. Among the genes with the highest expression ratios 1 day after sowing compared to fully mature seeds were genes identified as encoding amylase as well as enzymes involved in reduction (Table 2). Three days after sowing, the genes involved in respiration and photosynthesis such as ferredoxin and chlorophyll-binding protein were identified among the genes with the highest expression ratios.

Fe, Zn, Mn, and Cu localization changes during rice seed germination

To examine the localization of the metal ions (Fe, Zn, Mn, and Cu) during germination, we performed μ-XRE analysis in germinating seeds prior to radicle protrusion (i.e., the germination stage). Rice seeds were removed from agar plates without nutrients and sliced 12 h, 24 h, and 36 h after sowing. The

Accesion No.		signal intensities				ratio			Gene name	Proposed specificity
		0d	1d	2d	3d	1d	2d	3d		
AK099474	Os05g0316100								ZIP	Zinc
AK066887	Os05g0316100								ZIP	Zinc
AK105607	Os08g0467400								ZIP	Zinc
AK070501	Os08g0467400								ZIP	Zinc
AK102279	Os08g0467400								ZIP	Zinc
AK068640	Os02g0196000								OsZupT	Zinc
AK069804	Os04g0613000								OsZIP3	Zinc
AK100735	Os05g0128400								OsZAT(CDF family)	Zinc
AK064840	Os01g0837800								CDF family	Manganese
AK065961	Os03g0226400								CDF family	Manganese
AK110750	Os02g0775100								CDF family	Manganese
AK060150	Os01g0130000								CDF family	Manganese
AK061853	Os01g0130000								CDF family	Manganese
AK069315	Os01g0130000								CDF family	Manganese
AK107235	Os06g0700700								ATPase	Zinc
AK100988	Os02g0196600								ATPase	Copper
AK071310	Os02g0695800								OPT family	
AK070036	Os01g0142800								OPT family	
AK070216	Os04g0597600								OPT family	
AK102404	Os03g0751100								OPT family	
AK068351	Os12g0638200								OPT family	
AK101480	Os04g0597800								OPT family	
AK072617	Os06g0127700								OPT family	
AK060510	Os12g0638200								OPT family	
AK070801	Os04g0594800								OPT family	
AK072608	Os08g0320200								OPT family	
AK101055	Os10g0470700								OPT family	
AK064899	Os06g0706400								OPT family	
AK100112	Os07g0100600								OPT family	
AK072127	Os06g0125500								OPT family	
AK100814	Os08g0492000								OPT family	
AK070804	Os03g0719900								OPT family	
AK061822	Os07g0603800								OPT family	
AK101099	Os07g0603800								OPT family	
AK063490	Os06g0560000								Ferroportin/IREG	Iron
AK064831	Os12g0562100								Ferroportin-like	
AK065844	Os12g0562100								Ferroportin-like	
AK066049	Os03g0755100								IDI7	
AK109387	Os02g0187600								Os-PIC1	Iron
AK073270	Os06g0638100								Os-PIC2	Iron
AK107843	Os01g0138100								OsCOPT1	Copper
AK109200	Os01g0770800								OsCOPT2	Copper
AK104963	Os09g0440700								OsCOPT3	Copper
AK059730	Os04g0463400								OsVIT1	Iron
AK100055	Os06g0690700								RAN1	Zinc
AK072990	Os04g0556000								RAN1	Copper
AK063759	Os04g0556000								RAN1	Copper
AK101556	Os03g0216700								OsFRDL1	Iron-citrate
AK101612	Os10g0206800								OsFRDL2	
AK072077	Os10g0206800								OsFRDL2	
AK059217	Os08g0486100								PAA1	Copper
AK109176	Os03g0296600								ECA1	Manganese

Fig. 1 Expression patterns of metal transporter genes during seed germination. *Red* indicates upregulation, *blue* indicates downregulation, and *yellow* indicates signal intensities greater than 1,000

Table 1 Genes whose signal intensities were highest in mature seeds or in seeds 1–3 days after sowing

Accession No.		putative gene identification	signal				ratio		
			0d	1d	2d	3d	1d	2d	3d
0d signal intensity top10									
AK105251		unknown	445767	179673	174707	127529		0.39	0.29
AK106985		unknown	444962	179237	174692	109857		0.39	0.25
AK069098	Os01g0256500	Ramy1/Zn-induced protein	444068	179683	174717	87523		0.39	0.20
AK107328	Os07g0214300	Seed allergenic protein RAG3 precursor	442510	179674	134477	76747		0.30	0.17
AK059254		mitochondrial 26S ribosomal RNA.	441182	177478	127110	71921	0.40	0.29	0.16
AK061547		mitochondrial 26S ribosomal RNA.	439616	176904	113079	62779	0.40	0.26	0.14
AK107285		glutelin type I	438242	178564	106751	49802	0.41	0.24	0.11
AK063682	Os04g0589800	Late embryogenesis abundant (LEA) group 1 family pr	424455	176360	59630	12200	0.42	0.14	0.03
AK105037		Oryza sativa translation initiation factor (GOS2)	416364	176677	68565	28766	0.42	0.16	0.07
AK063517	Os11g0454200	Dehydrin RAB 16B	406856	135922	19414	5800	0.33	0.05	0.01
1d signal intensity top10									
AK073614		glycine-rich RNA-binding protein (OsGRP1)	270997	181090	176324	131474		0.65	0.49
AK069098	Os01g0256500	Ramy1/Zn-induced protein	444068	179683	174717	87523		0.39	0.20
AK107328	Os07g0214300	Seed allergenic protein RAG3 precursor	442510	179674	134477	76747		0.30	0.17
AK105251		unknown	445767	179673	174707	127529		0.39	0.29
AK106985		unknown	444962	179237	174692	109857		0.39	0.25
AK060454		unknown	246574	179066	142070	135946	0.73	0.58	0.55
AK060207		unknown	397226	178678	148029	92185	0.45	0.37	0.23
AK107285		glutelin type I	438242	178564	106751	49802	0.41	0.24	0.11
AK061298	Os10g0450800	Glycine-rich cell wall structural protein 2 precursor	250720	178457	137236	126312	0.71	0.55	0.50
AK062296		putative clathrin coat assembly protein	311264	178284	123771	78052	0.57	0.40	0.25
2d signal intensity top10									
AK071613	Os12g0555500	Probenazole-inducible protein PBZ1	47512	84568	188128	146534	**1.78**	**3.96**	**3.08**
AK108220	Os02g0452700	unknown	166406	147536	178722	121736			0.73
AK061042	Os06g0726200	Endochitinase precursor (EC 3.2.1.14)	19370	54627	178692	123771	**2.82**	**9.23**	**6.39**
AK105083	Os08g0129800	ribosomal protein 41	212159	160402	177219	132954		0.84	0.63
AK073614		glycine-rich RNA-binding protein (OsGRP1)	270997	181090	176324	131474		0.65	0.49
AK069098	Os01g0256500	Ramy1/Zn-induced protein	444068	179683	174717	87523		0.39	0.20
AK105251		unknown	445767	179673	174707	127529		0.39	0.29
AK106985		unknown	444962	179237	174692	109857		0.39	0.25
AK058529	Os05g0111300	Plant metallothionein, family 15 protein	92846	74777	171868	141135	0.81	**1.85**	**1.52**
AK061894	Os02g0121300	Peptidyl-prolyl cis-trans isomerase (Cyclophilin) (EC 5	82415	76795	161635	142487	0.93	**1.96**	**1.73**
3d signal intensity top10									
AK071613	Os12g0555500	Probenazole-inducible protein PBZ1	47512	84568	188128	146534	**1.78**	**3.96**	**3.08**
AK061894	Os02g0121300	Peptidyl-prolyl cis-trans isomerase (Cyclophilin) (EC 5	82415	76795	161635	142487	0.93	**1.96**	**1.73**
AK058529	Os05g0111300	Plant metallothionein, family 15 protein	92846	74777	171868	141135	0.81	**1.85**	**1.52**
AK060454		unknown	246574	179066	142070	135946	0.73	0.58	0.55
AK105083	Os08g0129800	ribosomal protein 41	212159	160402	177219	132954		0.84	0.63
AK073614		glycine-rich RNA-binding protein (OsGRP1)	270997	181090	176324	131474		0.65	0.49
AK105251		unknown	445767	179673	174707	127529		0.39	0.29
AK061298	Os10g0450800	Glycine-rich cell wall structural protein 2 precursor	250720	178457	137236	126312	0.71	0.55	0.50
AK058313	Os01g0200700	Metallothionein-like protein type 3 (MT-3)	44189	31239	145191	126052	0.71	**3.29**	**2.85**
AK061042	Os06g0726200	Endochitinase precursor (EC 3.2.1.14)	19370	54627	178692	123771	**2.82**	**9.23**	**6.39**

Bold indicates upregulation, *grey* indicates downregulation

samples were freeze-dried and used for X-ray imaging. The elemental maps of each element are presented for the half-sliced rice seeds (Fig. 2) and the enlarged images of the embryo (Fig. 3). Twelve hours after sowing, Fe accumulated in the dorsal vascular bundle, aleurone layer, and the endosperm (Fig. 2). In the embryo, Fe accumulated in the scutellum facing the endosperm near the ventral vascular bundle and the vascular bundle of the scutellum 12 h after sowing (Fig. 3). Twenty-four hours after sowing, Fe was still detectable in the dorsal vascular bundle. In the embryo, Fe distribution was dispersed in the scutellum, and had accumulated in the coleoptile. Fe accumulation in the epithelium and endosperm near the scutellum was also observed. Thirty-six hours after sowing, Fe was detected in the root tips. In the embryo, Fe was observed not only in epithelium, scutellum, and coleoptile, but also in the leaf primordium and radicle.

Zn was most abundant in the embryo. Zn was also distributed in the endosperm and was most abundant in the aleurone layer (Fig. 2). After sowing, Zn in the endosperm decreased compared to Zn in the embryo. In the embryo, high levels of Zn accumulated in the radicle and leaf primordium (Fig. 3). Twenty-four hours after sowing, Zn accumulation increased in the scutellum and the vascular bundle of the scutellum. In

Table 2 Genes whose expression ratios were highest in mature seeds or in seeds 1–3 days after sowing

Accession No.		putative gene identification	signal				ratio		
			0d	1d	2d	3d	1d	2d	3d
1d ratio top10									
AK102122	Os07g0639000	Peroxidase 1	571	5436	10396	4263	**9.52**	**18.20**	**7.46**
AK103316	Os09g0367700	GST6 protein (EC 2.5.1.18)	3552	33427	63675	41925	**9.41**	**17.92**	**11.80**
AK109664	Os09g0502500	Zinc-containing alcohol dehydrogenase superfamily pr	1598	13159	8751	3159	**8.23**	**5.48**	**1.98**
AK106714	Os08g0452500	Auxin responsive SAUR protein family protein	358	2943	2919	2022	**8.22**	**8.15**	**5.64**
AK058477	Os08g0434300	Malate dehydrogenase precursor (EC 1.1.1.37)	1077	8046	7471	6791	**7.47**	**6.94**	**6.31**
AK067632	Os01g0926300	Transaldolase (EC 2.2.1.2)	718	4826	2384	3642	**6.72**	**3.32**	**5.07**
AK108652	Os04g0662400	Auxin responsive SAUR protein family protein	53	348	717	207	**6.53**	**13.46**	**3.89**
AK063796	Os01g0369700	Glutathione S-transferase GST 8 (EC 2.5.1.18)	1395	9015	12232	9707	**6.46**	**8.77**	**6.96**
AK062619	Os04g0635000	Conserved hypothetical protein.	1026	6158	11565	2781	**6.00**	**11.27**	**2.71**
AK101744	Os02g0765600	Alpha-amylase precursor (EC 3.2.1.1)	1256	7434	23408	51931	**5.92**	**18.64**	**41.35**
2d ratio top10									
AK070056	Os01g0944700	Glucan endo-1,3-beta-glucosidase GII precursor (EC 3	1830	8068	67240	49441	**4.41**	**36.75**	**27.02**
AK103553	Os04g0339400	Aldo/keto reductase family protein	155	139	4229	6562	0.90	**27.37**	**42.47**
AK070443	Os01g0291500	Transferase family protein	207	104	4603	6714	0.50	**22.24**	**32.44**
AK064360	Os05g0134700	Haem peroxidase, plant/fungal/bacterial family protein	182	208	4027	1779	1.14	**22.16**	**9.79**
AK108025	Os05g0507000	Conserved hypothetical protein	133	145	2947	2930	1.09	**22.16**	**22.03**
AK062381	Os10g0552800	RCc3 protein	401	901	8458	6386	**2.25**	**21.09**	**15.92**
AK072862	Os07g0676900	Peroxidase (EC 1.11.1.7)	819	2634	16963	9567	**3.22**	**20.71**	**11.68**
AK060341	Os01g0251400	Hypothetical protein	679	1867	12985	20778	**2.75**	**19.13**	**30.61**
AK101744	Os02g0765600	Alpha-amylase precursor (EC 3.2.1.1)	1256	7434	23408	51931	**5.92**	**18.64**	**41.35**
AK060340	Os12g0114800	Nonspecific lipid-transfer protein 3 precursor (LTP 3)	3267	5692	60083	103292	**1.74**	**18.39**	**31.62**
3d ratio top10									
AK061619	Os01g0600900	Chlorophyll a-b binding protein 2 (LHCII type I CAB-2)	1038	65	10093	61669	0.06	**9.72**	**59.41**
AK058271	Os02g0731600	Thioredoxin-related domain containing protein	130	46	1853	6079	0.36	**14.28**	**46.85**
AK103553	Os04g0339400	Aldo/keto reductase family protein	155	139	4229	6562	0.90	**27.37**	**42.47**
AK071685	Os04g0459500	GADPH (383 AA) (Fragment)	196	43	1692	8172	0.22	**8.62**	**41.64**
AK101744	Os02g0765600	Alpha-amylase precursor (EC 3.2.1.1)	1256	7434	23408	51931	**5.92**	**18.64**	**41.35**
AK070261	Os02g0740400	Lipolytic enzyme, G-D-S-L family protein	202	209	999	8219	1.03	**4.95**	**40.74**
AK071989	Os04g0644400	Proline-rich-like protein	555	196	2299	21868	0.35	**4.14**	**39.41**
AK062438	Os07g0555200	Eukaryotic translation initiation factor 4G	1111	170	12734	42030	0.15	**11.46**	**37.83**
AK061654	Os08g0104600	Ferredoxin I, chloroplast precursor (Anti-disease protei	932	99	11929	33153		**12.80**	**35.56**
AK069955	Os11g0439600	Nod factor binding lectin-nucleotide phosphohydrolase	256	99	2783	9044		**10.87**	**35.32**

Bold indicates upregulation, *grey* indicates downregulation

the scutellum, Zn accumulated in the endosperm similarly to Fe. After 36 h, Zn was distributed in the leaf primordium and the root tip. Zn was also detected in a specific area that was assumed to be the junction between the embryo and the dorsal vascular bundle.

Mn was accumulated in the endosperm and embryo (Fig. 2). In the embryo, Mn accumulation in the scutellum decreased after sowing, whereas accumulation in the coleoptile increased (Fig. 3). Thirty-six hours after sowing, Mn was also observed in the root tip.

Cu is also an important element for plants, but its concentration in the plant body is extremely low. Using the SPring-8 facilities, we succeeded in detecting Cu in the rice seed. Cu was detected not only in the embryo but also in the endosperm (Figs. 2 and 3). After sowing, Cu in the scutellum decreased and accumulation in the coleoptile and root were observed.

To examine the localization of the transporter gene involved in the mobilization of stored Zn during germination, promoter-GUS fusion activity was analyzed in germinating seeds. We monitored the promoter activity of *OsZIP4*, which encodes a Zn transporter (Fig. 4). *OsZIP4* expression was observed in fully mature seeds in the bud scale, coleorhizae, vascular bundle of the scutellum, and leaf primordium (Fig. 4a). Upon germination, *OsZIP4* expression was induced in the dorsal vascular bundle (Fig. 4b). In the embryo, *OsZIP4* expression was strongly induced in the vascular bundle of the scutellum (Fig. 4c, d). Three days after sowing, *OsZIP4* expression was storongly observed in the scutellum, the vascular bundle of the scutellum, coleoptile, and radicle (Fig. 4d).

Discussion

Metal transporters are involved in metal flow during rice seed germination

Using microarray analysis, we found that many transporter genes were strongly expressed and that their expression levels changed during rice seed

germination (Fig. 1). These results suggested that localization of metal ions is regulated at the molecular level. Genes involved in seed protein storage and the gene annotated as the Zn-induced protein were included in the list of genes having the highest signal intensities in mature seeds and in seeds 1 day after sowing (Table 1). Note that this Zn-induced protein is also identified as the Zn-finger protein, RAMY, which binds to the α-amylase gene and is probably involved in its gibberellin-induced expression (Peng et al. 2004). Expression of these genes decreased dramatically during seed germination. This tendency suggested that genes important in the first phase of seed germination need to be downregulated during the latter stages of seed germination, and Zn may play an important role here. During the 2–3 days after sowing, the gene encoding metallothionein was upregulated. Metallothionein is reported to be involved in metal translocation (Fukuzawa et al. 2004; Zhou et al. 2006), suggesting that metal translocation is important during seed germination. One day after sowing, the genes for amylase and enzymes involved in reduction and were upregulated (Table 2). Starch degradation triggered by plant hormones was suggested to occur during this period. Since metal nutrients are important as cofactors for some enzymes, metal translocation might be important for these enzyme activities. Three days after sowing, genes involved in respiration and photosynthesis such as ferredoxin and the chlorophyll-binding protein were induced. These data suggest that proteins abundant in seeds decrease 1–2 days after sowing and biological functions such as respiration become active 3 days after sowing. Furthermore, metals, especially Fe and Zn, are suggested to be important for these activities. In our microarray results, many transporter genes thought to be involved in metal transport were expressed at high levels during rice seed germination (Fig. 1). Genes encoding ZIP family members putatively involved in Zn transport decreased during seed germination (Nozoye et al. 2007; Fig. 1). This trend was observed for the most abundant genes in mature seeds, which were downregulated during seed germination (Table 1). In the μ-XRE Zn imaging analysis, Zn accumulation in meristematic tissues was limited in the embryo (Figs. 2 and 3). A decrease in OsZIP family transcripts might be necessary for this type of partial localization of Zn. Similarly to other members of the rice ZIP family genes, *OsZIP4* expression in whole seeds decreased in the 2–3 days after sowing. *OsZIP4* promoter-GUS activity in the embryo, however, was strong and did not decrease during seed germination (Fig. 4). Therefore, expression in specific tissues and downregulation in other parts of the seed might be important for specific Zn translocation.

Free Fe ion is extremely toxic to plants, as it injures cells by catalyzing the generation of cellular free radicals. Therefore, small-molecule chelators have been speculated to be required for the utilization of the Fe. Mugineic acid family phytosiderophores (MAs) are natural Fe chelators that graminaceous plants secrete from their roots to solubilize Fe in the soil (Takagi 1976). As MAs have been identified in the xylem and phloem of rice and barley (Mori et al. 1991; Kawai et al. 2001), MAs may play an important role in the long-distance transport of Fe in graminaceous plants as well. Nicotianamine (NA), an intermediate in the MA biosynthetic pathway, is also thought to be involved in the long-distance transport of metal cations in the plant body (Stephan and Scholz 1993; Higuchi et al. 1996; Pich and Scholz 1996; Stephan et al. 1996; Ling et al. 1999; Takahashi et al. 2003). Moreover, NA has been suggested to play an essential role in metal translocation and accumulation in developing seeds, based on analysis of NA-deficient transgenic tobacco (Nicotiana tabacum) plants (Takahashi et al. 2003). Rice produces and secretes deoxymugineic acid (DMA), the initial compound synthesized in the MA biosynthetic pathway. We recently suggested that DMA and NA are involved in Fe transport during rice seed germination based on results from promoter-GUS and microarray analysis (Nozoye et al. 2007). We previously reported that genes not obviously induced under Fe-deficient conditions in vegetative tissues are strongly expressed during seed germination (Nozoye et al. 2007). Among the three nicotianamine synthase genes in rice (*OsNAS1–3*), *OsNAS3*, the gene least induced under Fe deficiency in roots (Inoue et al. 2003), was found to be most abundantly expressed during rice seed germination (Nozoye et al. 2007). Similar tendencies were observed for the expression of metal transporters during rice seed germination. For example, *OsNramp2* and *OsFRDL1* expression were strongly induced during germination, even though these genes were not induced under Fe-deficient conditions. Different regulatory mechanisms may be operating in expression during rice seed germination compared to that under nutrient-deficient conditions.

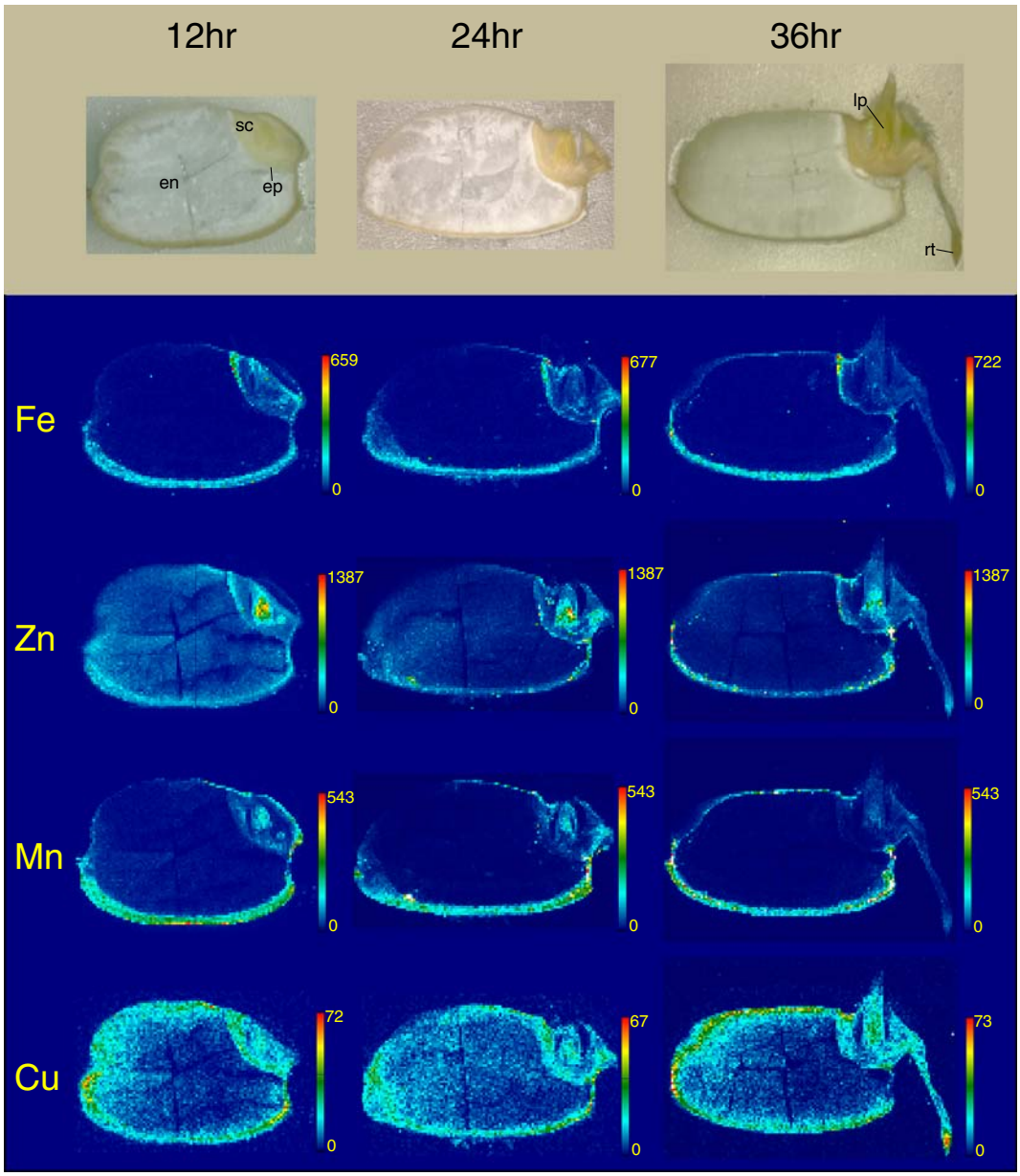

Fig. 2 The elemental maps of Fe, Zn, Mn, and Cu in half-sliced germinating rice seeds. The normalized X-ray fluorescence intensities are scaled from *red* (maximum) to *blue* (minimum). Each image indicates the relative distribution of the specific element, and thus the concentration scale varies for each image. sc, scutellum; en, endosperm; lp, leaf primordium; rp, root tip; ep, epithelium

Translocation of metal nutrients (Fe, Zn, Mn, and Cu) during rice seed germination involves NA and DMA

Using μ-XRE analysis at the SPring-8 facility, we have for the first time succeeded in documenting the changes in distribution of Fe, Mn, Zn, and Cu during rice seed germination (Figs. 2 and 3). Changes in distribution showed distinct patterns between the elements. Several regulatory mechanisms were suggested to exist for metal homeostasis during rice seed germination.

Most of the Fe in fully mature rice seeds is associated with the embryo and the aleurone layer (Fig. 2); Fe distribution in the scutellum increased

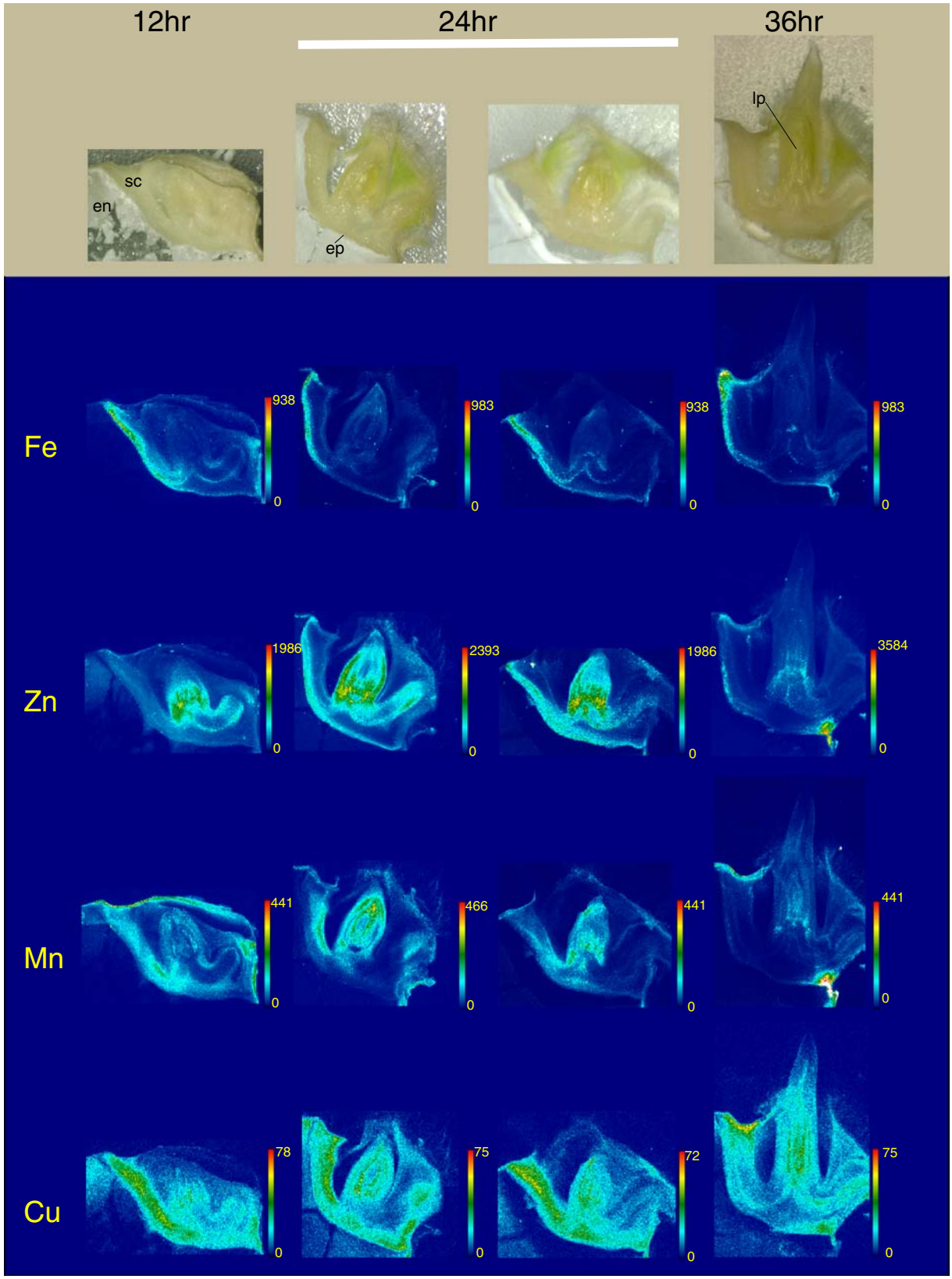
12hr
24hr
36hr
sc
en
ep
lp
Fe
938
0
983
0
938
0
983
0
Zn
1986
0
2393
0
1986
0
3584
0
Mn
441
0
466
0
441
0
441
0
Cu
78
0
75
0
72
0
75
0

◀ **Fig. 3** The elemental maps of Fe, Zn, Mn, and Cu in the embryo of the germinating rice seeds. The normalized X-ray fluorescence intensities are scaled from *red* (maximum) to *blue* (minimum). Each image shows the relative distribution of the specific element, and thus the concentration scale varies for each image. sc, scutellum; en, endosperm; lp, leaf primordium; ep, epithelium

after sowing. Recently, we hypothesized that Fe stored in the endosperm was transported into the scutellum through the epithelium, collected into the vascular bundle of the scutellum, and then transported to the leaf primordium and seminal root based on promoter–GUS analysis of the genes involved in DMA synthesis and Fe transport (Nozoye et al. 2007). Fe localization visualized by SPring-8 in the present study strongly supports our hypothesis that DMA and NA are involved in Fe transport from the aleurone to the leaf primordium and seminal root. NA is thought to be produced because *OsNAS2* is expressed in the endosperm (Nozoye et al. 2007). However, Fe concentrations were highest in the aleurone layer, but not throughout the endosperm (Fig. 2). DMA and NA also have the ability to chelate Zn, Mn, and Cu (von Wirén et al. 1999), suggesting their role in transporting these metals during rice seed germination.

Zn accumulated in the whole endosperm (Fig. 2). NA was suggested to have an important role in Zn mobilization in the endosperm. Fe is associated with ferritin or phytate in the endosperm. Zn accumulated in the endosperm is associated not only with phytate, but also with protein (Cakmak et al. 2004). The differences in metal distribution might suggest the differences of their storage form. Zn flow was quite dynamic compared to other metals analyzed. Zn stored in the endosperm was transported to the scutellum and collected in the vascular bundle of the scutellum and then transported to the seminal root and leaf primordium (Figs. 2 and 3). Zn accumulation in the junction between the embryo and the dorsal vascular bundle increased after sowing. The dorsal vascular bundle seemed to be the route of Zn transport to the embryo. Zn is the most critical micronutrient affecting protein synthesis in plants (Cakmak et al. 1989; Obata et al. 1999). In actively growing root and shoot meristematic tissues, Zn is most likely utilized in protein synthesis, membrane structure and function, gene expression, and oxidative stress tolerance (Cakmak 2000). High Zn concentrations in newly developed tissues were confirmed to be important during rice seed germination.

Mn distribution in the endosperm was similar to that of Fe (Fig. 2), and Cu distribution in the endosperm was similar to that of Zn (Fig. 2). This similarity might be related to the differences in storage forms. Following sowing, distribution of Mn and Cu had spread to the scutellum and increased in the seminal root and leaf primordium. In the scutellum, the accumulation of Mn and Cu decreased, and the accumulation in the coleoptile and root increased. The possibility exists that Mn and Cu in the embryo are actively used for growth of the coleoptile and radicle during seed germination, and flow from the endosperm to embryo was not as active compared to Fe and Zn.

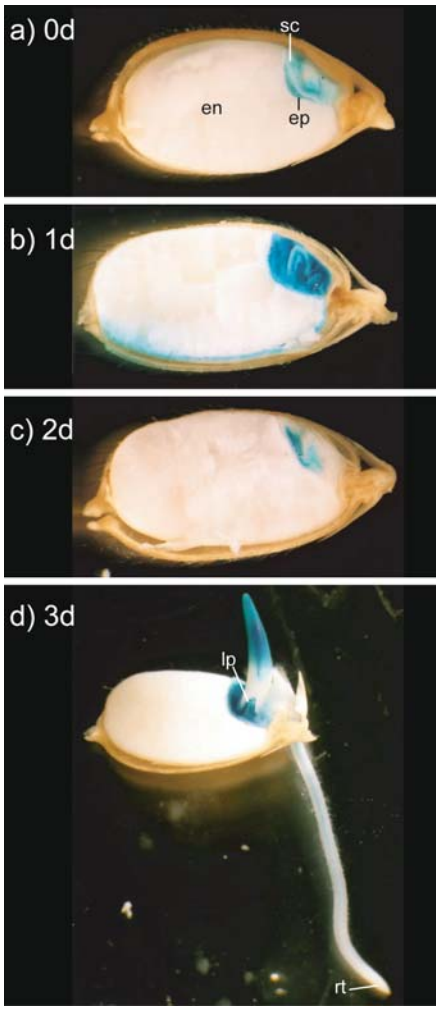

Fig. 4 Histochemical localization of GUS activity derived from *OsZIP4* promoter-GUS transformants in fully mature seeds (**a**, 0 days) and seeds 1–3 days (**b**–**d**) after sowing. sc, scutellum; en, endosperm; lp, leaf primordium; rp, root tip; ep, epithelium

In conclusion, we succeeded in visualizing the Fe, Zn, Cu, and Mn flow during rice seed germination for the first time. Fe, Zn, Cu, and Mn flow were different from each other, and NA and DMA were suggested to be involved in their flow during rice seed germination.

Acknowledgements We thank Dr Khurram Bashir for reading manuscript and helpful discussions, and Dr Yoshiaki Nagamura of the Rice Genome Project and the NIAS DNA Bank (National Institute of Agrobiological Sciences, Tsukuba, Japan) for support with the 22 K oligo array analysis.

References

Axelaen KB, Palmgren MG (2001) Inventory of the superfamily of P-type ion pumps in *Arabidopsis*. Plant Physiol 126:696–706

Cakmak I (2000) Role of zinc in protecting plant cells from reactive oxygen species. New Phytol 146:185–205

Cakmak I, Marschner H, Bangerth F (1989) Effect of zinc nutritional status on growth, protein metabolism and levels of indole-3-acetic acid and other phytohormones in bean (*Phaseolus vulgaris* L.). J Exp Bot 40:405–412

Cakmak I, Torun A, Millet E, Feldman M, Fahima T, Korol A, Nevo E, Braun HJ, Ozkan H (2004) *Triticum dicoccoides*: an important genetic resource for increasing zinc and iron concentration in modern cultivated wheat. Soil Sci Plant Nutr 50:1047–1054

Clemens S (2006) Toxic metal accumulation, responses to exposure and mechamisms of tolerance in plants. Biochimie 88:1707–1719

Colangelo EP, Guerinot ML (2006) Put the metal to the petal: metal uptake and transport throughout plants. Curr Opin Plant Biol 9:322–330

Curie C, Panaviene Z, Loulergue C, Dellaporta SL, Briat J-F, Walker EL (2001) Maize yellow stripe encodes a membrane protein directly involved in Fe(III) uptake. Nature 409:364–349

Durrett TP, Gassmann W, Rogers EE (2007) The FRD3-mediated efflux of citrate into the root vasculature is necessary for efficient iron translocation. Plant Physiol 144:197–205

Duy D, Wanner G, Meda AR, von Wiren N, Soll J, Philippar K (2007) PIC1, an ancient permease in Arabidopsis chlorplasts, mediates iron transport. Plant Cell 19:986–1006

Eide D, Broderius M, Fett J, Guerinot ML (1996) A novel iron-regulated metal transporter from plants identified by functional expression in yeast. Proc Natl Acad Sci U S A 28:5624–8

Finney LA, O'Halloran TV (2003) Transition metal speciation in the cell: insights from the chemistry of metal ion receptors. Science 300:931–936

Fukuzawa H, Yu L-H, Umeda-Hara C, Tagawa M, Uchimiya H (2004) The rice metallothionein gene promoter does not direct foreign gene expression in seed endosperm. Plant Cell Rep 23:231–235

Grotz N, Guerinot ML (2006) Molecular aspects of Cu, Fe and Zn homeostasis in plants. Biochim Biophys Acta 1763:595–608

Hell R, Stephan UW (2003) Iron uptake, trafficking and homeostasis in plants. Planta 216:541–551

Hiei Y, Ohta S, Komari T, Kumashiro T (1994) Efficient transformation of rice (Oryza sativa L.) mediated by Agrobacterium and sequence analysis of the boundaries of the T-DNA. Plant J 6:271–82

Higuchi K, Nishizawa NK, Romheld V, Marschner H, Mori S (1996) Absence of nicotinamine synthase activity in the tomato mutant 'chloronerva'. J Plant Nutr 19:1235–1239

Higuchi K, Suzuki K, Nakanishi H, Yamaguchi H, Nishizawa NK, Mori S (2001) Nicotianamine synthase gene expression differs in barley and rice under Fe-deficient conditions. Plant J 25:159–167

Hirayama T, Kieber JJ, Hirayama N, Kogan M, Guzman P, Nourizadeh S, Alonso JM, Dailey WP, Dancis A, Ecker JR (1999) Responsive-to-antagonist 1, a Menkes/Wilson disease-related copper transporter, is required for ethylene signaling in *Arabidopsis*. Cell 97:383–393

Hokura A, Onuma R, Kitajima N, Nakai I, Terada Y, Abe T, Saito H, Yoshida S (2006) In: Proc. 8th Int. Conf. X-ray Microscopy, IPAP Conf. Series 7, pp. 323–325

Hoshikawa K (1973) Theory and practices of raising paddy rice seedlings for mechanized transplanting. 6. Agri & Hort 48:1253–1254

Huang C, Barker SJ, Langridge P, Smith FW, Graham RD (2000) Zinc deficiency up-regulates expression of high-affinity phosphate transporter genes in both phosphate-sufficient and–dficient barley roots. Plant Physiol 124:415–422

Hydon M, Cobbett CS (2007) Transporters of ligands for essential metal ions in plants. New Phytol 174:499–506

Inoue H, Higuchi K, Takahashi M, Nakanishi H, Mori S, Nishizawa NK (2003) Three rice nicotianamine synthase genes, OsNAS1, OsNAS2, and OsNAS3 are expressed in cells involved in long-distance transport of iron and differentially regulated by iron. Plant J 36:366–81

Ishimaru Y, Suzuki M, Tsukamoto T, Suzuki K, Nakazono M, Kobayashi T, Wada Y, Watanabe S, Matsuhashi S, Takahashi M, Nakanishi H, Mori S, Nishizawa NK (2006) Rice plants take up iron as an Fe^{3+}-phytosiderophore and as Fe^{2+}. Plant J 45:335–346

Jefferson RA, Kavanagh TA, Bevan NM (1987) GUS fusion: b-glucuronidase as a sensitive and versatile gene fusion marker in higher plants. EMBO J:63901–63907

Kamijo N, Suzuki Y, Takano H, Tamura S, Yasumoto M, Takeuchi A, Awaji M (2003) Rev Sci Instrum 74:5101

Kampfenkel K, Kushnir S, Babiychuk E, Inzé D, Van Montagu M (1995) Molecular characterization of a putative Arabidopsis thaliana copper transporter and its yeast homologue. J Biol Chem 270:48479–28486

Kawai S, Kamei S, Matsuda Y, Ando R, Kondo S, Ishizawa A, Alam S (2001) Concentrations of iron and phytosiderophores in xylem sap of iron-deficient barley plants. Soil Sci Plant Nutr 47:265–272

Kim SA, Punshon T, Lanzirotti A, Li L, Alonzo JM, Ecker JR, Kaplan J, Guerinot ML (2006) Localization of iron in Arabidopsis seed requires the vacuolar membrane transporter VIT1. Science 314:1295–1298

Korshunova YO, Eide D, Clark WG, Guerinot ML, Pakrasi HB (1999) The IRT1 protein from Arabidopsis thaliana is a metal transporter with a broad substrate range. Plant Mol Biol 40:37–44

Krämer U, Talke IN, Hanikenne M (2007) Transition metal transport. FEBS letters 581:2263–2272

Ling HQ, Koch G, Baumlein H, Ganal MW (1999) Map-based cloning of chloronerva, a gene involved in iron uptake of higher plants encoding nicotianamine synthase. Proc Natl Acad Sci U S A 96:7098–103

McKie AT, Marciana P, Rolfs A, Brennan K, Wehr K, Barow D, Miret S, Bomford A, Peters TJ, Farzaneh F, Hediger MA, Hentze MW, Simpson RJ (2000) A novel duodenal iron-regulated transporter, IREG1, implicated in the basolateral transfer of iron to the circulation. Mol Cell 5:299–309

Mills RF, Krijger GC, Baccarini PJ, Hall JL, Williams LE (2003) Functional expression of AtHMA4, a P_{1B}-type ATPase in the Zn/Co/Cd/Pb subclass. The Plant Journal 35:164–175

Mori S, Nishizawa NK, Hayashi H, Chino M, Yoshimura E, Ishihara J (1991) Why are young rice plants highly susceptible to iron deficiency? Plant and Soil 130:143–156

Nozoye T, Inoue H, Takahashi M, Ishimaru Y, Nakanishi H, Mori S, Nishizawa NK (2007) The expression of iron homeostasis-related genes during rice germination. Plant Mol Biol 64:35–47

Obata H, Kawamura S, Senoo K, Tanaka A (1999) Changes in the level of protein and activity of Cu/Zn-superoxide dismutase in zinc deficient rice plant, *Oryza sativa* L. Soil Sci Plant Nutr 45:891–896

Peng R, Yao Q, Xiong A, Fan H, Li X, Peng Y, Cheng ZM, Li Y (2004) A new rice zinc-finger protein binds to the O2S box of the alpha-amylase gene promoter. Eur J Biochem 271:2949–55

Pich A, Scholz G (1996) Translocation of copper and other micronutrients in tomato plants (Lycopersion esculentum Mill.): Nicotianamine-stimulated copper transport in the xylem. J Exp Bot 294:41–47

Pittman JK (2005) Managing the manganese: molecular mechanisms of manganese transport and homeostasis. New Phytol 167:733–742

Puig S, Andress-Colas N, Garcia-Molina A, Penarrubia L (2007) Copper and iron homeostasis in Arabidopsis: responses to metal deficiencies, interactions and biotechnological applications. Plant Cell Environ 30:271–290

Schaaf G, Honsbein A, Meda AR, Kirchner S, Wipf D, von Wirén N (2006) AtIREG2 encodes a tonoplast transport protein involved in iron-dependent nickel detoxification in Arabidopsis thaliana roots. J Biol Chem 281:25532–40

Shikanai T, Müller-Moulé P, Munekage Y, Niyogi KK, Pilon M (2003) PAA1, a P-type ATPase of *Arabidopsis*, functions in copper transport in chloroplasts. The Plant Cell 15:1333–1346

Stephan UW, Scholz G (1993) Nicotianamine: Mediator of transport of iron and heavy metals in the phloem? Physiol Plant 88:522–529

Stephan UW, Schmidke I, Stephan VW, Scholz G (1996) The nicotianamine molecule is made-tomeasure for complexation of metal micronutrients in plants. Biometals 9:84–90

Takagi S (1976) Naturally occurring iron-chelating compounds in oat- and rice-root washings. I. Activity measurement and preliminary characterization. Soil Sci Plant Nutr 45:993–1002

Takahashi M, Terada Y, Nakai I, Nakanishi H, Yoshimura E, Mori S, Nishizawa NK (2003) Role of nicotianamine in the intracellular delivery of metals and plant reproductive development. Plant Cell 15(6):1263–80

Takaiwa F, Kikuchi S, Oono K (1987) A rice glutelin family-A major type of glutelin mRNAs can be devised into two classes. Mol Gen Genet 208:15–22

Vert G, Grotz N, Dedaldechamp F, Gaymard F, Guerinot ML, Briat JF, Curie C (2002) IRT1, an Arabidopsis transporter essential for iron uptake from the soil and for plant growth. Plant Cell 14:1223–33

von Wirén N, Klair S, Bansal S, Briat JF, Khodr H, Shioiri T, Leigh RA, Hider RC (1999) Nicotianamine chelates both FeIII and FeII. Implications for metal transport in plants. Plant Physiol 119:1107–1114

Williams LE, Mills RF (2005) P(1B)-ATPase-an ancient family of transition metal pumps with diverse function in plants. Trends Plant Sci 10:491–502

Williams LE, Pittman JK, Hall JL (2000) Emerging mechanisms for heavy metal transport in plants. Biochimica et Biophysica Acta 1465:104–126

Woeste KE, Kieber JJ (2000) A strong loss- function mutation in *RAN1* results in constitutive activation of the ethylene response pathway as well as a rosette-lethal phenotype. The Plant Cell 12:443–455

Yamagichi H, Nishizawa NK, Nakanishi H, Mori S (2002) IDI7, a new iron-regulated ABC transporter from barley roots, localizes to the tonoplast. J Experi Botany 53:727–735

Zhou G, Xu Y, Lingyan JL, Liu J-Y (2006) Molecular Analysis of the Metallothonein Gene Family in Rice (*Oryza sativa* L.). J Biochem Mol Biol 39:595–606